Coupling of Cortical Hemodynamic Response to Neuronal Activity in Cortex and Thalamus

642.11

Anna Devor[1], Istvan Ulbert[1,2], Andrew K Dunn[1], Suresh N Narayanan[1], Mark L Andermann[1], David A Boas[1] and Anders M Dale[1,3]

[1]MGH-NMR Center, Harvard Medical School, Charlestown, MA [2]Institute for Psychology of the Hungarian Academy of Sciences, Budapest, Hungary [3]Departments of Neurosciences and Radiology, University of California, San Diego, CA

Summary

Accurate interpretation of functional magnetic resonance imaging (fMRI) signals requires knowing the relationship between changes in the hemodynamic response and neuronal activity that underlies it. Here we address the question of coupling between pre- and post-synaptic neuronal activity, and the hemodynamic response in rodent somatosensory (Barrel) cortex in response to deflection of a single whisker. Using full-field multi-wavelength optical imaging of hemoglobin oxygenation combined with electrophysiological recordings of spiking and synaptic neuronal activity we demonstrate that (a) a point hemodynamic measure is influenced by neuronal activity across multiple cortical columns, and (b) the oxy- and total-hemoglobin hemodynamic responses can be well approximated by space-time separable functions with an antagonistic center-surround spatial pattern extending over several millimeters. The surround "negative" hemodynamic activity did not correspond to observable changes in neuronal activity. This work demonstrates for the first time that the hemodynamic response is not just a temporal convolution of the neuronal activation, but is also a spatial convolution. Thus, attempts at characterizing the neurovascular relationship based on point measurements of electrophysiology and hemodynamics may yield inconsistent results, depending on the spatial extent of neuronal activation. The finding that the hemodynamic signal observed at a given location is a function of electrophysiological activity over a broad spatial region helps explain a previously observed nonlinearity in the neurovascular relationship. The complex spatial integration of the hemodynamic response should be considered when interpreting fMRI data in terms of neuronal activity.

Spatiotemporal evolution of the hemodynamic response

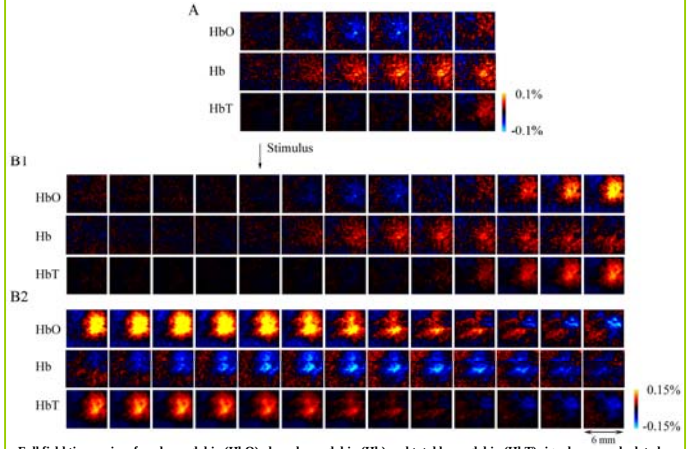

Full field time series of oxyhemoglobin (HbO), deoxyhemoglobin (Hb) and total hemoglobin (HbT) signals were calculated from 6 wavelength data. Each image represents an individual frame (average of ~1400 trials). Time between consecutive images is 200 msec. Panel B2 is a continuation of the time series shown in panel B1. The signal for Hb and HbO is expressed in percent change relative to its own baseline concentration (40 and 60 mM respectively). HbT was calculated as a sum of Hb and HbO. The arrow denotes stimulus delivery. The time period of the initial dip is repeated on a different intensity scale in A.

The hemodynamic response has an antagonistic center-surround spatial pattern

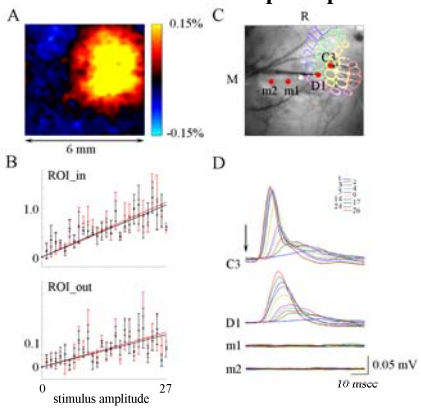

A. An image of HbO at the peak of the response.

B. Integral HbO (red) and HbT (black) responses as a function of stimulus intensity in the center (principal barrel, ROI_in) and surround (>3mm away from the recording electrode, ROI_out). Data from 5 animals were averaged, all amplitudes are shown. The error bars reflect the inter-subject standard error. The center and surround response amplitudes in every animal were normalized to the maximal response amplitude in the center ROI for that animal before averaging the data across animals. Note that the magnitude of the negative surround response is in average ~10% of that in the center.

C. The locations of electrophysiological recordings are superimposed on the image of the vasculature corresponding to the functional map in A. Recordings from locations m1 and m2 were performed following recordings from C3 and D1 barrels (the electrodes are visible on the image). An approximate location of the Barrel field was drawn using C3 and D1 penetration sites, and the Barrel field size as spatial constraints.

D. Electrophysiological responses recorded from each of the four locations marked in C. Responses to different stimulus amplitudes (inset) are superimposed. The arrow denotes stimulus delivery. Note that m1 and m2 locations (C) correspond to the region of the surround negativity.

HbO and HbT responses are space-time separable

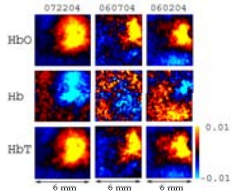

PCA analysis was performed on each one of the hemodynamic parameters (HbO, Hb and HbT) across time and amplitudes. Three examples of spatial patterns of the first PCA component for HbO, Hb and HbT are illustrated. The percentage of variance explained is listed in table below. The case ID for each animal is denoted on top.

Case ID	HbO	Hb	HbT
72204	94.00%	76.00%	95.00%
72604	79.00%	42.00%	85.00%
60704	70.00%	36.00%	82.00%
60104	68.00%	35.00%	76.00%
60204	85.00%	58.00%	87.00%

The local hemodynamic response increases beyond saturation of local neuronal activity

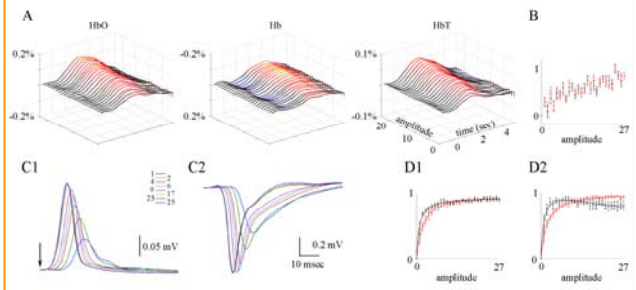

A. Timecourses of HbO, Hb and HbT averaged from 300x300 μm ROI around the electrode recording from the principal barrel. The data were averaged from 8 animals and smoothed using 5 amplitudes sliding window. 5 of the 8 animals are shown in the previous (PCA) figure.

B. Integral HbO (red) and HbT (black) responses as a function of stimulus intensity. Data from the same 8 animals were averaged, all amplitudes are shown. The error bars reflect the inter-subject standard error.

C. An example of MUA (C1) and LFP (C2) responses. Responses to different amplitudes (inset) are superimposed. The arrow denotes stimulus delivery.

D. MUA (D1) and LFP (D2) peak (red) and integral (black) responses as a function of stimulus amplitude. The data were averaged across the same subjects as in A/B. The curves were fitted using the function ax/(1-bx)c.

Thalamic VPM and cortical responses saturate with an increase in stimulus intensity

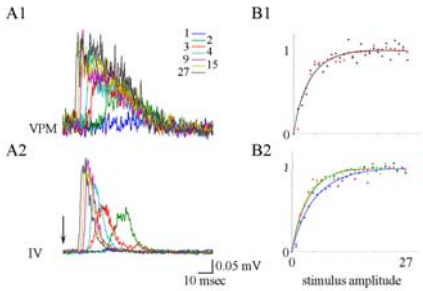

A. MUA activity was recorded simultaneously in thalamus (VPM) using a single metal electrode and in the cortex using a laminar electrode array. Responses for different stimulus amplitudes (inset) are superimposed for VPM (top) and cortical layer IV (bottom). An input impedance of recording electrodes, 7 MW in the VPM and 0.2 MW in the cortex, explains differences in signal-to-noise ratio.

B1. VPM (blue) and cortical layer IV (red) peak response as a function of stimulus intensity. The curves were fitted using the function ax/(1-bx)c.

B2. Granule (layer IV, red), supra-granule (blue) and infra-granule (green) peak responses as a function of stimulus amplitude.

Neither lemniscal or paralemniscal inputs increase beyond saturation of the post-synaptic activity

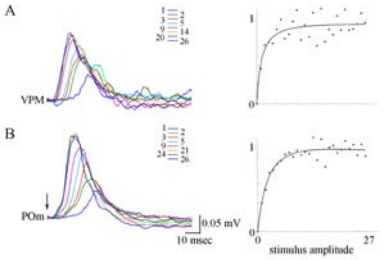

MUA activity was simultaneously recorded from VMP and POm using two laminar electrode arrays. Responses for different stimulus amplitudes (inset) are superimposed for VPM (A) and POm (B). The peak response as a function of stimulus intensity was fitted using the function ax/(1-bx)c.

Neuronal activity in surround cortical columns increases throughout

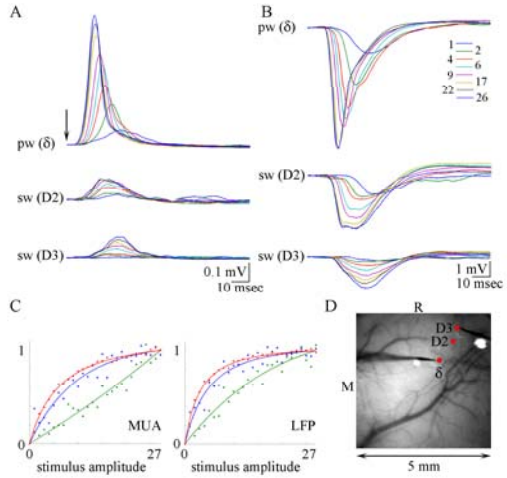

MUA (A) and LFP (B) responses are plotted for the principal barrel (δ) and two surround barrels (D2 and D3). Responses to different amplitudes (inset) are superimposed. The arrow denotes stimulus delivery.

C. MUA (left) and LFP (right) peak responses as a function of stimulus amplitude. The curves were fitted using the function ax/(1-bx)c.

D. Locations of electrophysiological recordings are superimposed on the image of the vasculature. Recordings from barrel columns δ and D3 (the electrodes are visible on the image) were performed following recordings from δ and D2 barrels.

Methods

Rats were initially anesthetized with 1.5% halothane and ventilated with ~ 1% halothane in mixture of air and oxygen. Halothane was discontinued, and anesthesia was maintained with 50 mg*kg-1 intravenous bolus of a-chloralose followed by continuous intravenous infusion at 40 mg*kg-1*h-1. An area of skull overlying the primary somatosensory cortex was exposed and thinned. A small hole was made in the thinned skull, and the recording electrode was introduced through the dura matter. For recordings involving laminar probes the thinned skull and dura matter were removed.

To illuminate the cortex, light from a mercury xenon arc lamp was directed through a 6-position rotating filter wheel (560, 570, 580, 590, 600 and 610 nm) coupled to a 12 mm fiber bundle. Images of about 6 mm^2 area were acquired by cooled 12 bit CCD camera. The spectral data were converted to percent change maps for Hb, HbO and HbT using the modified Beer-Lambert law. Differential pathlength correction was applied to adjust for the differential optical pathlength through the tissue at different wavelengths.

Electrophysiological recordings were performed using either single metal microelectrodes or a linear array multielectrodes with 24 contacts spaced at 100 mm. The signals were amplified and filtered between 500-5000 Hz to record MUA, and between 0.1-500 Hz to record LFP. The MUA signals were rectified on the time axis before averaging. Averaged LFP curves were rectified on the time axis before integration. Cortical microelectrodes were positioned in lower layer II/III (400-500 mm).

Single whiskers were deflected upward by a wire loop coupled to a computer controlled piezoelectric stimulator. We employed a fast, randomized event-related stimulus presentation paradigm analogous to that used in event-related fMRI studies. The stimulation paradigm consisted of single deflections of varying amplitude with interstimulus interval (ISI) of 1 sec.